

ationdalvi $Aggregating_2013e@last43$

DATA AND DOMAIN UNCERTAINTY IN MACHINE LEARNING

by
Artin Majdi

A Dissertation Submitted to the Faculty of the
GRADUATE INTERDISCIPLINARY PROGRAM
IN APPLIED MATHEMATICS

In Partial Fulfillment of the Requirements
For the Degree of

DOCTOR OF PHILOSOPHY

In the Graduate College
THE UNIVERSITY OF ARIZONA

M a y 2 4 , 2 0 2 3

Get the official approval page
from the Graduate College
before your final defense.

STATEMENT BY AUTHOR

This dissertation has been submitted in partial fulfillment of requirements for an advanced degree at The University of Arizona and is deposited in the University Library to be made available to borrowers under rules of the Library.

Brief quotations from this dissertation are allowable without special permission, provided that accurate acknowledgment of source is made. Requests for permission for extended quotation from or reproduction of this manuscript in whole or in part may be granted by the head of the major department or the Dean of the Graduate College when in his or her judgment the proposed use of the material is in the interests of scholarship. In all other instances, however, permission must be obtained from the author.

SIGNED: _____

DEDICATION

For God.

ACKNOWLEDGMENTS

First and foremost, thanks go to co-advisors Anna Mehmbuhr and Mbaqanga Uffda. Much of what I have learned in this project has been learned through them; their patience has been endless and their knowledge has been irreplaceable. Susan Kho and Vincenzo Mitti, as well, have given me valuable feedback as I have revised my dissertation this spring.

Summer 2009, fall 2009, and spring 2010 research assistantships were funded by the University of Arizona Department of Mathematics NSF VIGRE (Vertical InteGration in Research and Education) grant. The remaining semesters of my PhD years were funded by teaching assistantships. I thank my college-algebra, trigonometry, and calculus students for helping me to see mathematics from both sides of the classroom.

TABLE OF CONTENTS

LIST OF FIGURES

LIST OF TABLES

[illegible]

LIST OF TABLES—*CONTINUED***0.1 Introduction**

Supervised learning techniques require a large amount of labeled data to train models to classify new data [Jiang et al., 2019a, Jiang et al., 2019b]. Traditionally, data labeling has been assigned to experts in the domain or well-trained annotators [Tian et al., 2019]. Although this method produces high-quality labels, it is inefficient and costly [Li et al., 2016, Li et al., 2019]. Social networking provides an innovative solution to the labeling problem by allowing data to be labeled by online crowd annotators. This has become feasible, as crowdsourcing services such as Amazon Mechanical Turk (formerly CrowdFlower) have grown in popularity. Crowdsourcing systems have been used to accumulate large amounts of labeled data for applications such as computer vision [Deng et al., 2009, Liu et al., 2012] and natural language processing [Karger et al., 2014]. However, because of individual differences in preferences and cognitive abilities, the quality of labels acquired by a single crowd annotator is typically low, thus jeopardizing applications that rely on these data. This is because crowd annotators are not necessarily domain experts and may lack the necessary training or expertise to produce high-quality labels. Aggregation after repeated labeling is one method for handling annotators with various abilities. Label aggregation is a process used to infer an aggregated label for a data instance from a multi-label set [Sheshadri and Lease, 2013]. Several studies have demonstrated the efficacy of repeated labeling [Tu et al., 2018, Zhang and Wu, 2018]. Repeat labeling is a technique in which the same data are labeled by multiple annotators, and the results are combined to estimate an aggregated label using majority voting (MV) or other techniques. In the case of MV, an aggregated label is the label that receives the most votes from the annotators for a given data instance. This can help reduce the impact of biases or inconsistencies made by annotators. Several factors, such as problem-specific characteristics, the quality of the labels created by the annotators, and the amount of data available, can influence the effectiveness of the aggregation methodologies. Consequently, it is difficult to identify a clear winner among the different techniques. For example, in binary labeling, one study [Sheshadri and Lease, 2013] discovered that Raykar’s [Raykar et al., 2010] technique outperformed other aggregation techniques. However, according to another study [Zheng et al., 2017], the traditional Dawid-Skene (DS) model [Dawid and Skene, 1979] was more reliable in multi-class settings (where data instances can be labeled as belonging to multiple classes). Furthermore, regardless of the aggregation technique used, the performance of many aggregation techniques in real-world datasets remains unsatisfactory [Liu et al., 2021]. This can be attributed to the complexity of these datasets, which often do not align with the assumptions and limitations of different methods. For example, real-world datasets may present issues such as labeling inaccuracies, class imbalances, or overwhelming sizes that challenge efficient processing with available resources. These factors can

LIST OF TABLES—*CONTINUED*

adversely affect the effectiveness of label aggregation techniques, potentially yielding less than optimal results for real-world datasets. Prior information may be used to enhance the label aggregation procedure. This can include domain knowledge, the use of quality control measures and techniques that account for the unique characteristics of annotators and data. Knowing the reliability of certain annotators, it is possible to draw more accurate conclusions about labels [Li et al., 2017]. For instance, in the label aggregation process, labels produced by more reliable annotators (such as domain experts) may be given greater weight. The results of the label aggregation process can also be validated using expert input [Liu et al., 2017]. During the labeling process, domain experts can provide valuable guidance and oversight to ensure that the labels produced are accurate and consistent. The agnostic requirement for general-purpose label aggregation is that label aggregation cannot use information outside the labels themselves. This requirement is not satisfied in most label aggregation techniques [Zhang et al., 2019]. The agnostic requirement ensures that the label aggregation technique is as general as possible and applicable to a wide range of domains with minimal or no additional context. The uncertainty of annotators during labeling can provide valuable prior knowledge to determine the appropriate amount of confidence to grant each annotator while still adhering to the requirement of a general-purpose label aggregation technique. We developed a method for estimating the reliability of different annotators based on the annotator’s own consistency during labeling and their accuracy with respect to other annotators. We propose a novel method called “crowd-certain”, which provides a more accurate aggregation of labels, ultimately leading to improved overall performance in both crowdsourcing and ensemble learning scenarios. The experimental results show that the proposed technique generates a weight that closely follows the annotator’s degree of reliability. Furthermore, the proposed method uses the consistency and accuracy of annotators as a measure of their reliability relative to other annotators. Experiments performed on a variety of crowdsourcing datasets indicate that the proposed method outperforms prior methods in terms of accuracy with a significant improvement over all investigated benchmarks (Gold Majority Vote, MV, MMSR, Wawa, Zero-Based Skill, GLAD, and Dawid Skene), particularly when few annotators are available.

The remainder of this paper is organized as follows. Section 2 examines related work involving label aggregation algorithms. In Section 3, we provide a detailed explanation of our proposed technique. Section 4 presents the experiments and findings. Finally, Section 5 summarizes the findings and identifies the main directions for future research.

0.2 Related Work

Numerous label aggregation algorithms have been developed to capture the complexity of crowdsourced labeling systems, including techniques based on annotator reliability [Bi et al., 2014, Demartini et al., 2012], confusion matrices [Raykar et al., 2010, Zhang et al., 2014], intentions [Bi et al., 2014, Kurve et al., 2015], biases [Zhang et al., 2013, Hernandez-Gonzalez et al., 2019, Welinder et al., 2010], and correlations [Ma et al., 2020]. However, because crowdsourced labeling is inherently dynamic and uncertain, developing a technique that can work in most situations is extremely challenging. Many techniques [Liu et al., 2012, Karger et al., 2014, Raykar et al., 2010, Dalvi et al., 2013, Ghosh et al., 2011] utilize the Dawid and Skene (DS) generative model [Dawid and Skene, 1979]. Ghosh [Ghosh et al., 2011] extended the DS model by using singular value decomposition (SVD) to calculate the reliability of the annotator. Similarly to Ghosh [Ghosh et al., 2011], Dalvi [Dalvi et al., 2013] used SVD to estimate true labels with a focus on the sparsity of the labeling matrix. In crowdsourcing, it is common for the labeling matrix to be sparse, meaning that not all annotators have labeled all the data. This may be due to several factors, such as the cost of labeling all data instances or the annotators’ time constraints. Karger [Karger et al., 2014] described an iterative strategy for binary labeling based on a one-coin model [Ghosh et al., 2011]. Karger [Karger et al., 2014] extends the one-coin model to multi-class labeling by converting the problem into $k-1$ binary problems (solved iteratively), where k is the number of classes. The MV technique assumes that all annotators are equally reliable. For segmentation, Warfield [Warfield et al., 2004] proposed simultaneous truth and performance level estimation (STAPLE), a label fusion method based on expectation maximization. STAPLE “weighs” expert opinions during label aggregation by modeling their reliability. Since then, many variants of this technique have been proposed [Winzeck et al., 2018, Commowick et al., 2018, Asman and Landman, 2011, Asman and Landman, 2012, Eugenio Iglesias et al., 2013, Jorge Cardoso et al., 2013, Asman and Landman, 2013, Akhondi-Asl et al., 2014]. The problem with these label aggregation approaches is that they require the computation of a unique set of weights for each sample, necessitating the re-evaluation of the annotators’ weights when a new instance is added. Among the numerous existing label aggregation strategies, MV remains the most efficient and widely used approach [Tao et al., 2020]. If we assume that all annotators are equally reliable and that their errors are independent of one another, then, according to the theory of large numbers, the likelihood that the MV is accurate increases as the number of annotators increases. However, the assumption that all annotators are equally competent and independent may not always hold. Furthermore, MV does not provide any additional information on the degree of disagreement among the annotators (As an example, consider the scenario where four of seven doctors think patient A needs

LIST OF TABLES—*CONTINUED*

immediate surgery, while all seven think patient B needs immediate surgery; MV will simply label “yes” in both cases). To address this problem, additional measures such as inter-annotator agreement (IAA) have been used [Artstein, 2017]. IAA is a measurement of the agreement among multiple annotators who label the same data instance. Typically, IAA is calculated using statistical measures, such as Cohen’s kappa, Fleiss’s kappa, or Krippendorff’s alpha [Krippendorff, 2018]. These measures consider both the observed agreement between the annotators and the expected agreement owing to random chance. IAA can also be visualized using a confusion matrix or annotation heatmap, which illustrates the distribution of labels assigned by the annotators. This can help identify instances where the annotators disagree or are uncertain and can guide further analysis to improve the annotation [Carletta, 1996]. Recently, Sheng [Sheng et al., 2019] proposed a technique that provided a confidence score along with an aggregated label. The main problem with this approach is that it assumes that all annotators are equally capable when calculating the confidence score. Tao [Tao et al., 2020] improved Sheng’s approach by assigning different weights to annotators for each instance. This weighting method combines the specific quality $s_\alpha^{(i)}$ for the annotator α and instance i and the overall quality τ_α across all instances. Inspired by Li’s technique [Li et al., 2018], Tao evaluates the similarity between the annotator labels for each instance. To derive the specific quality $s_\alpha^{(i)}$, Tao counts the number of annotators who assigned the same label as the annotator α for that instance. To calculate the overall quality τ_α , Tao performs a 10-fold cross-validation to train each of the 10 classifiers on a different subset of data using the labels provided by the annotator α as true labels and then assigns the average accuracy across all remaining instances as τ_α . The final weight for annotator α and instance i is then calculated using the sigmoid function $\gamma_{i,\alpha} = \tau_\alpha \left(1 + \left(s_\alpha^{(i)} \right)^2 \right)$. However, Tao’s technique [Tao et al., 2020] has some drawbacks. It relies on the labels of other annotators to estimate $s_\alpha^{(i)}$. However, different annotators have varying levels of competence (reliability) when labeling the data, and therefore, relying on their labels to measure $s_\alpha^{(i)}$ will result in propagating the errors and biases of their labels during weight estimation. Furthermore, Tao’s technique [Tao et al., 2020] relies on the labels provided by each annotator α to estimate their respective τ_α by assuming that the trained classifiers can learn the inherent characteristics of the datasets even in the absence of ground truth labels. While that may be true in some cases, it typically leads to suboptimal measurement and the propagation of biases and errors, from both the annotator’s labels and the classifier, into weight estimation.

LIST OF TABLES—*CONTINUED***0.3 Methods**

We propose a novel method called “crowd-certain” which focuses on leveraging uncertainty measurements to improve decision-making in crowdsourcing and ensemble learning scenarios. Crowd-Certain employs a weighted soft majority voting approach, where the weights are determined based on the uncertainty associated with each annotator’s labels. Initially, we use uncertainty measurement techniques to calculate the degree of consistency of each annotator during labeling. Furthermore, to ensure that the proposed technique does not calculate a high weight for annotators who are consistently wrong (for example, when a specific annotator always mislabels a specific class, and hence demonstrates a high consistency while having low accuracy), we extend the proposed technique by penalizing the annotators for instances in which they disagree with the aggregated label obtained using the MV. To mitigate the reliance on training a classifier on an annotator’s labels, which may be inaccurate, we train an ensemble of classifiers for each annotator. In addition, we report two confidence scores along with the aggregated label to provide additional context for each calculated aggregate label. We report a single weight for all instances in the dataset. As demonstrated in the experimental sections, the proposed crowd-certain method is not only comparable to other techniques in terms of accuracy for scenarios with a large number of annotators, but also provides a significant improvement in accuracy for scenarios where the number of annotators may be limited. Furthermore, by assigning a single weight to each annotator for all instances in the dataset, the model can assign labels to new test instances without recalculating the annotator weights. This is especially advantageous in situations where annotators are scarce as it enables the model to make accurate predictions with minimal dependence on the annotator input. This characteristic of the crowd-certain method can significantly reduce the time and resources required for labeling in practical applications. When deploying the model in real-world scenarios such as medical diagnosis, fraud detection, or sentiment analysis, it could be advantageous to be able to assign labels to new instances without constantly recalculating annotator weights.

0.3.1 Glossary of Symbols

Let us denote the following parameters:

N : Number of instances.

M : Number of annotators.

$y_k^{(i)} \in \{0, 1\}$: True label for the k -th class for instance i .

$z_{\alpha,k}^{(i)} \in \{0, 1\}$: Label given by annotator α for k -th class for instance i .

LIST OF TABLES—*CONTINUED*

$MV_{\alpha}^{(i)}(z_{\alpha,k}^{(i)})$: Majority voting technique (the label that receives the most votes) applied to annotator labels for class k and instance i .

$\pi_{\alpha,k}$: Reliability score to generate sample labels for annotator α for class k . For example, it may be obtained from a uniform distribution in the interval 0.4 to 1, i.e., $\pi_{\alpha,k} \sim U(0.4, 1)$.

$X^{(i)}$: Data for instance i .

$Y^{(i)} = \{y_1^{(i)}, y_2^{(i)}, \dots, y_K^{(i)}\}$: True label set, for instance i . For example, consider a dataset that is labeled for the presence of cats, dogs, and rabbits in any given instance. If a given instance $X^{(i)}$ has cats and dogs but not rabbits, then $Y^{(i)} = \{1, 1, 0\}$.

$Z_{\alpha}^{(i)} = \{z_{\alpha,1}^{(i)}, z_{\alpha,2}^{(i)}, \dots, z_{\alpha,K}^{(i)}\}$: Label set given by the annotator α for instance i .

K : number of categories (aka classes) in a multi-class multi-label problem. For example, if we have a dataset labeled for the presence of cats, dogs, and rabbits in any given instance, then $K = 3$.

$\rho^{(i)}$: Randomly generated number between 0 and 1 for instance i . It is obtained from a uniform distribution, i.e., $\rho^{(i)} \sim U(0, 1)$. This number will be used to determine, for each instance i , whether the true label should be assigned to each fictitious annotator's label. For each class k if the annotator's reliability score for that class $\pi_{\alpha,k}$ is greater than $\rho^{(i)}$, the true label $y_k^{(i)}$ will be assigned; otherwise, an incorrect label $1 - y_k^{(i)}$ will be assigned.

$\Pi_{\alpha} = \{\pi_{\alpha,1}, \pi_{\alpha,2}, \dots, \pi_{\alpha,K}\}$: set of K reliability scores for annotator α .

$\mathbb{X} = \{X^{(i)}\}_{i=1}^N$: Set of all instances.

$\mathbb{Y} = \{Y^{(i)}\}_{i=1}^N$: Set of all true labels.

$\mathbb{Z}_{\alpha} = \{Z_{\alpha}^{(i)}\}_{i=1}^N$: Set of all labels for the annotator α .

$\widehat{\mathbb{Y}} = \{\widehat{Y}^{(i)}\}_{i=1}^N$: Set of all aggregated labels.

$\mathbb{P} = \{\rho^{(i)}\}_{i=1}^N$: Set of N randomly generated numbers.

$\mathbb{D} = \{\mathbb{X}, \mathbb{Y}\}$: Dataset containing all instances and all true labels.

LIST OF TABLES—*CONTINUED*

$\mathbb{D}_\alpha = \{\mathbb{X}, \mathbb{Z}_\alpha\}$: Dataset containing the labels given by the annotator α .

$\mathbb{D}_\alpha^{\text{train}}, \mathbb{D}_\alpha^{\text{test}}$: Train and test crowd datasets randomly selected from \mathbb{D}_α where $\mathbb{D}_\alpha^{\text{train}} \cup \mathbb{D}_\alpha^{\text{test}} = \mathbb{D}_\alpha$ and $\mathbb{D}_\alpha^{\text{train}} \cap \mathbb{D}_\alpha^{\text{test}} = \emptyset$

$F_\alpha^{(g)}(\cdot)$: Classifier g trained on dataset $\mathbb{D}_\alpha^{\text{train}}$ with random seed number g (which is also the classifier index)

$P_\alpha^{(i,g)} = \left\{ p_{\alpha,k}^{(i,g)} \right\}_{k=1}^K$: Predicted probability set obtained in the output of the classifier $F_\alpha^{(g)}(\cdot)$ representing the probability that each class k is present in the sample.

$\theta_{\alpha,k}^{(g)}$: Binarization threshold. To obtain this, we can utilize any existing thresholding technique (for example, in one technique, we analyze the ROC curve and find the corresponding threshold where the difference between the true positive rate (sensitivity) and false positive rate (1-specificity) is maximum; Alternatively, we could simply use 0.5).

$t_{\alpha,k}^{(i,g)} = \begin{cases} 1 & \text{if } p_{\alpha,k}^{(i,g)} \geq \theta_{\alpha,k}^{(g)} \\ 0 & \text{otherwise.} \end{cases}$: Predicted label obtained by binarizing $p_{\alpha,k}^{(i,g)}$.

$\eta_{\alpha,k}^{(i)} = \text{MV}_g(t_{\alpha,k}^{(i,g)})$: The output of the majority vote applied to the predicted labels obtained by the G classifiers.

$u_{\alpha,k}^{(i)}$: Uncertainty score.

$c_{\alpha,k}^{(i)}$: Consistency score.

$\omega_{\alpha,k}$: Estimated weight for annotator α and class k .

$v_k^{(i)} = \frac{1}{M} \sum_\alpha \omega_{\alpha,k} \eta_{\alpha,k}^{(i)}$: Final aggregated label for class k and instance i .

0.3.2 Risk Calculation

Label aggregation is frequently used in various machine learning tasks, such as classification and regression, when multiple annotators assign labels to the same data points. The aggregation model refers to the underlying function that maps a set of multiple labels obtained by different annotators, into one aggregated label. In the context of label aggregation, this model can be a neural network, a decision tree, or any other machine learning algorithm capable of learning to aggregate labels provided by multiple annotators. The objective of this study is to develop an aggregation

LIST OF TABLES—*CONTINUED*

model capable of accurately determining true labels despite potential disagreements among annotators. One common method to achieve this involves minimizing the total error (or disagreement) between the annotators’ assigned labels and the true labels, as follows:

$$E = \sum_{i=1}^N \sum_{a=1}^M \left(\sum_{k=1}^K \delta \left(y_k^{(i)}, z_{a,k}^{(i)} \right) \right) \quad (0.3.1)$$

where δ is the Kronecker delta function.

Although error is a crucial aspect in determining the aggregation model’s performance, it treats false positives and false negatives with equal weight. However, in many practical scenarios, it is essential to weigh false positives and false negatives differently depending on the specific context and potential consequences of each type of misclassification. The concept of risk allows us to achieve this by incorporating a loss function, which assigns different weights to different types of errors. In this way, risk serves as a weighted calculation of error, enabling us to better evaluate the performance of an aggregation model and its generalization capability.

Let us denote loss function, $\mathcal{L}(\cdot)$, as a function that quantifies the discrepancy between the predicted labels and the true labels, accounting for the varying importance of different types of errors. Risk, denoted as $R(h)$, represents the expected value of a loss function over the entire dataset, capturing the performance of the aggregation model on all possible data instances. In practice, our goal is to minimize the risk to achieve optimal performance on unseen data. However, since we only have access to a limited dataset (empirical distribution), we instead work with the empirical risk. This limitation may arise because of the need to reserve a portion of our data for testing and validation or because no dataset can fully capture all possible data instances in the real world. However, minimizing risk alone could result in overfitting, in which the aggregation model learns the noise in the training data rather than the underlying patterns, resulting in poor generalization to unseen data. To improve generalizability, it is necessary to employ regularization techniques to strike a balance between the complexity of the aggregation model and its ability to fit the training data.

Risk measurement enables us to assess the aggregation model’s performance in terms of accuracy, overfitting (when risk is minimized but the model performs poorly on unseen data), and model complexity.

Assume that the aggregation model $h(\cdot)$ is a function that takes a set of M label sets $Z^{(i)}$ for each instance i in the training data and calculates an aggregated label set $\hat{Y}^{(i)}$ as an estimate of the true label set $Y^{(i)}$. Our goal is to find an aggregation model $h(\cdot)$ that minimizes risk as follows:

LIST OF TABLES—*CONTINUED*

$$R(h) = \frac{1}{N} \sum_{i=1}^N \mathcal{L} \left(Y^{(i)}, h \left(\left\{ Z_{\alpha}^{(i)} \right\}_{\alpha=1}^M \right) \right) \quad (0.3.2)$$

In this context, $\mathcal{L}(\cdot)$ represents an arbitrary loss function, which quantifies the discrepancy between predicted labels and true labels while accounting for the varying importance of different types of errors.

Our goal is to choose an aggregation model \hat{h} that minimizes the risk, following the principle of risk minimization [Vapnik, 1991], as shown below:

$$\hat{h} = \underset{h}{\operatorname{argmin}} R(h) \quad (0.3.3)$$

0.3.3 Generating Annotators' Label Sets from Ground Truth

In order to evaluate the proposed crowd-certain technique (with and without penalization) as well as other aggregation techniques, we create M fictitious annotators. To synthesize a multi-annotator dataset from a dataset with existing ground truth, we use a uniform distribution in the interval from 0.4 to 1, i.e., $\pi_{\alpha,k} \sim U(0.4, 1)$ (however other ranges can also be used) to obtain $M \times K$ reliability values Π , where K is the number of classes. (Note that an annotator may be skilled at labeling dogs, but not rabbits.) Then we use these reliability values to generate the crowd label set $Z_{\alpha}^{(i)}$ from the ground truth labels for each instance i .

For each annotator α , each instance i and class k in the dataset is assigned its true label with probability $\pi_{\alpha,k}$ and the opposite label with probability $(1 - \pi_{\alpha,k})$. To generate the labels for each annotator α , a random number $0 < \rho^{(i)} < 1$ is generated for each instance i in the dataset. Then $\forall \alpha, k$ if $\rho^{(i)} \leq \pi_{\alpha,k}$ then the true label is used for that instance and class for the annotator α ; otherwise, the incorrect label is used.

The calculated annotator labels $z_{\alpha,k}^{(i)}$ for each annotator α , instance i and class k are as follows:

$$z_{\alpha,k}^{(i)} = \begin{cases} y_k^{(i)} & \text{if } \rho^{(i)} \leq \pi_{\alpha,k}, \\ 1 - y_k^{(i)} & \text{if } \rho^{(i)} > \pi_{\alpha,k}, \end{cases} \quad \forall i, \alpha, k \quad (0.3.4)$$

To evaluate the proposed techniques over all data instances, a k-fold cross-validation is employed.

0.3.4 Uncertainty Measurement

A common approach to measure uncertainty is to increase the number of data instances X in the test dataset $\mathbb{D}_{\alpha}^{\text{test}}$ to create multiple variations of each sample data

LIST OF TABLES—*CONTINUED*

$X^{(i)}$ [Ayhan and Berens, 2018]. In this approach, for each instance i , we apply randomly generated spatial transformations and additive noise to the input data $X^{(i)}$ to obtain a transformed sample and repeat this process G times to obtain a set of G transformed samples. However, this approach is mostly suitable for cases where the input data is images or volume slices. Since the datasets used in this study consist of feature vectors instead of images or volume slices, this approach cannot be used. To address this problem, we introduced a modified uncertainty measurement approach, in which instead of augmenting the data instances $X^{(i)}$, we feed the same sample data to different classifiers. For the choice of classifier, we can either use a probability-based classifier such as random forest and train it under G different random states or train various classifiers and address the problem in a manner similar to ensemble learning (using a set of G different classification techniques such as random forest, SVM, CNN, Adaboost, etc.). In either case, we obtain a set of G classifiers $\left\{F_{\alpha}^{(g)}(\cdot)\right\}_{g=1}^G$ for each annotator α . The classifier $F_{\alpha}^{(g)}(\cdot)$ is a pre-trained or pre-designed model that has been trained on a labeled training dataset $\mathbb{D}_{\alpha}^{\text{train}}$. This training process enables $F_{\alpha}^{(g)}(\cdot)$ to learn the underlying patterns in the data and make predictions on unseen instances. After training, we feed the test samples $X^{(i)} \in \mathbb{X}^{\text{test}}$ to the g -th classifier $F_{\alpha}^{(g)}(\cdot)$ as test cases. The classifier $F_{\alpha}^{(g)}(\cdot)$ then outputs a set of predicted probabilities $\left\{p_{\alpha,k}^{(i,g)}\right\}_{k=1}^K$ representing the probability that class k is present in the sample. Consequently, we obtain a collection of G predicted probability sets $\left\{\left\{p_{\alpha,k}^{(i,g)}\right\}_{k=1}^K\right\}_{g=1}^G$ for each annotator α and instance i . The set $\left\{p_{\alpha,k}^{(i,g)}\right\}_{g=1}^G$ contains the predicted probabilities for class k , annotator α , and instance i . Disagreements between predicted probabilities $\left\{p_{\alpha,k}^{(i,g)}\right\}_{g=1}^G$ can be used to estimate uncertainty. The reason for using classifiers rather than using the crowdsourced labels directly is two-fold. Using a probabilistic classifier helps us calculate uncertainty based on each annotator’s labeling patterns that the classifier learns. Furthermore, this approach provides us with a set of pre-trained classifiers $\left\{\left\{F_{\alpha}^{(g)}(\cdot)\right\}_{g=1}^G\right\}_{\alpha=1}^M$ that can be readily utilized on any new data instances without the need for those samples to be labeled by the original annotators. The index value $g \in \{1, 2, \dots, G\}$ is used as the random seed value during training of the g th classifier for all annotators. Define $t_{\alpha,k}^{(i,g)}$ as the predicted label obtained by binarizing the predicted probabilities $p_{\alpha,k}^{(i,g)}$ using the threshold $\theta_{\alpha,k}^{(g)}$ as shown in the Glossary of Symbols section. Uncertainty measures are used to quantify the level of uncertainty or confidence associated with the predictions of a model. In this work,

LIST OF TABLES—CONTINUED

we need to measure the uncertainty $u_{\alpha,k}^{(i)}$ associated with the model predictions. Some common uncertainty measurement measures are as follows.

Entropy Entropy is a widely used measure of uncertainty in classification problems. In an ensemble of classifiers, entropy serves as a quantitative measure of the uncertainty or disorder present in the probability distribution of the predicted class labels. A higher entropy value indicates a greater degree of uncertainty in the predictions, as the predictions of the individual classifiers in the ensemble are significantly different. In contrast, a lower entropy value denotes reduced uncertainty as the ensemble assigns very similar probabilities to a particular class, indicating strong agreement among the classifiers and increased confidence in their collective prediction. The formula for calculating entropy is as follows:

$$u_{\alpha,k}^{(i)} = H\left(\left\{p_{\alpha,k}^{(i,g)}\right\}_{g=1}^G\right) = -\sum_g p_{\alpha,k}^{(i,g)} \log\left(p_{\alpha,k}^{(i,g)}\right) \quad (0.3.5)$$

Standard Deviation In regression problems, standard deviation is often used to quantify uncertainty. It measures the dispersion of predicted values around the mean. A greater standard deviation indicates greater uncertainty of the prediction. For a set of predicted values $\{t_{\alpha,k}^{(i,g)}\}_{g=1}^G$ with mean value μ , the standard deviation is defined as

$$u_{\alpha,k}^{(i)} = \text{SD}\left(\left\{t_{\alpha,k}^{(i,g)}\right\}_{g=1}^G\right) = \sqrt{\frac{1}{G-1} \sum_{g=1}^G \left(t_{\alpha,k}^{(i,g)} - \mu\right)^2}, \quad \mu = \frac{1}{G} \sum_{g=1}^G t_{\alpha,k}^{(i,g)} \quad (0.3.6)$$

Predictive Interval: A predictive interval provides a range within which a future observation is likely to fall with a certain level of confidence. For example, a 95% predictive interval indicates that there is a 95% likelihood that the true value falls within that range. A greater uncertainty corresponds to wider intervals. In the context of multiple classifiers, the predictive intervals can be calculated by considering the quantiles of the classifier output. For a predefined confidence level γ (e.g., 95%), for a specific class k , we need to find the quantiles Q_L^k and Q_U^k of the probability distribution of class k predicted by the G classifiers. The uncertainty can be represented by the width of the predictive interval:

$$\begin{aligned} P\left(Q_L^k \leq p_{\alpha,k}^{(i,g)} \leq Q_U^k\right) &= \gamma \\ u_{\alpha,k}^{(i)} &= Q_U^k - Q_L^k \end{aligned} \quad (0.3.7)$$

The steps to calculate the predictive interval are as follows:

LIST OF TABLES—*CONTINUED*

1. Collect the class k probabilities predicted by all G classifiers for a given instance. Then sort the values in ascending order. Let us call this set $P_{\alpha,k}^{(i)} = \text{sorted}\left(\left\{p_{\alpha,k}^{(i,g)}\right\}_{g=1}^G\right)$, $\forall \alpha, k, i$.
2. Calculate the lower and upper quantile indices based on the chosen confidence level γ . The lower quantile index is $L = \text{ceil}\left(\frac{G}{2}(1 - \gamma)\right)$, and the upper quantile index is $U = \text{floor}\left(\frac{G}{2}(1 + \gamma)\right)$, where ceil and floor are the ceiling and floor functions, respectively.
3. Find the values corresponding to the lower and upper quantile indices in the sorted $P_{\alpha,k}^{(i)}$. These values are the lower and upper quantiles Q_L^k and Q_U^k .
4. Now we have the predictive interval $P\left(Q_L^k \leq p_{\alpha,k}^{(i,g)} \leq Q_U^k\right) = \gamma$, where Q_L^k and Q_U^k represent the bounds of the interval containing the α proportion of the probability mass.

Monte Carlo Dropout The Monte Carlo dropout [Gal and Ghahramani, 2016] can be used to estimate uncertainty in neural networks by applying the dropout at test time. Multiple forward passes with dropout generate a distribution of predictions from which uncertainty can be derived using any of the aforementioned techniques (standard deviation, entropy, etc.).

Bayesian Approaches Bayesian methods offer a probabilistic framework to estimate the parameters of the model and make predictions. These methods explicitly model uncertainty by considering prior beliefs about the model parameters and then updating those beliefs based on the observed data. In Bayesian modeling, the model parameters are treated as random variables and a posterior distribution is estimated using these parameters. The following are two common Bayesian approaches for measuring the uncertainty in classification problems.

- **Bayesian model averaging (BMA):** BMA accounts for model uncertainty by combining the predictions of various models using their posterior probabilities as weighting factors. Instead of selecting a single “best” model, BMA acknowledges the possibility of multiple plausible models, each with its own strengths and weaknesses [Hoeting et al., 1999]. The steps to implement BMA are as follows. Select a set of candidate models that represent different hypotheses regarding the data-generating process underlying the data. These models may be of various types, such as linear regression, decision trees, neural networks,

LIST OF TABLES—*CONTINUED*

or any other model suited to the specific problem at hand. Using the available data, train each candidate model. Calculate the posterior probabilities of the models. Using the posterior probabilities of each model as weights, calculate the weighted average of each model’s predictions. The weighted average is the BMA prediction for the input instance and class.

- **Bayesian neural networks (BNNs):** BNNs [Mullachery et al., 2018] are an extension of conventional neural networks in which the weights and biases of the network are treated as random variables. The primary distinction between BNNs and conventional neural networks is that BNNs model uncertainty directly in the weights and biases. The posterior distributions of the network weights and biases (learned during training) capture the uncertainty, which can then be utilized to generate predictive distributions for each class. This enables multiple predictions to be generated by sampling these predictive distributions, which can be used to quantify the uncertainty associated with each class.

Committee-Based Methods Committee-based method [Wang et al., 2020] involves training multiple models (a committee) and aggregating their predictions. The disagreement between committee members’ predictions can be used as a measure of uncertainty. Examples include bagging and boosting ensemble methods and models, such as random forests.

$$u_{\alpha,k}^{(i)} = \text{VarCommittee} \left(P_{\alpha,k}^{(i)} \right) = \frac{1}{G} \sum_{g=1}^G \left(p_{\alpha,k}^{(i,g)} - \mu \right)^2, \quad \mu = \frac{1}{G-1} \sum_{g=1}^G p_{\alpha,k}^{(i,g)} \quad (0.3.8)$$

Conformal Prediction: Conformal prediction [Angelopoulos and Bates, 2021] is a method of constructing prediction regions that maintain a predefined level of confidence. These regions can be used to quantify the uncertainty associated with the prediction of a model.

Steps to calculate the nonconformity score:

[1.] For each classifier g and each class k , calculate the nonconformity score. Here, `score_function` measures the conformity of the prediction with the true label. In the context of this study, the true label can be replaced by $\eta_{\alpha,k}^{(i)}$. A common choice for `score_function` is the absolute difference between the predicted probability and the true label, but other options can be used depending on the specific problem and requirements. Define the nonconformity score as $\zeta_k^g = \text{score_function} \left(p_{\alpha,k}^{(i,g)}, y_k^{(i)} \right)$. Calculate the p-value pv_k for each class k as the proportion of classifiers with nonconformity scores greater than or equal to

LIST OF TABLES—*CONTINUED*

a predefined threshold T_k : $p\text{-values}(k) = \frac{|\{g: \zeta_k^g \geq T_k\}|}{G}$ The p-values calculated for each class k represent the uncertainty associated with that class. A higher p-value indicates a higher level of agreement among the classifiers for a given class, whereas a lower p-value suggests greater uncertainty or disagreement.

The uncertainty measures discussed above are only some of the available options. Selecting an appropriate measure depends on factors such as the problem domain, the chosen model, and the specific requirements of a given application. For this study, we use the variance technique shown in Equation (0.3.6) as our uncertainty measurement due to its simplicity. However, other measures could also be employed as suitable alternatives.

0.3.5 Crowd-Certain: Uncertainty-Based Weighted Soft Majority Voting

Consistency Measurement Define $c_{\alpha,k}^{(i)}$ as the consistency score for annotator α , class k and instance i . We calculate this consistency score using the uncertainty score $u_{\alpha,k}^{(i)}$ explained in the previous section. We use two approaches to calculate $c_{\alpha,k}^{(i)}$ from $u_{\alpha,k}^{(i)}$.

[1.]The first approach is to simply subtract the uncertainty from 1 as follows:

$$c_{\alpha,k}^{(i)} = 1 - u_{\alpha,k}^{(i)} \quad , \quad \forall i, \alpha, k \quad (0.3.9)$$

In a second approach (shown in Equation (0.3.10)), we penalize annotators for instances in which their predicted label $\eta_{\alpha,k}^{(i)}$ (explained in the Glossary of Symbols section) does not match the MV of all annotator labels $MV_{\alpha}(z_{\alpha,k}^{(i)})$. As previously discussed, instead of directly working with the annotator's labels $z_{\alpha,k}^{(i)}$, we use the predicted labels obtained from the ensemble of classifiers $\eta_{\alpha,k}^{(i)}$. This methodology does not require repeating the crowd-labeling process for new data samples. In particular, we are likely not to have access to the same crowd of annotators employed in the training dataset.

$$c_{\alpha,k}^{(i)} = \begin{cases} 1 - u_{\alpha,k}^{(i)} & \text{if } \eta_{\alpha,k}^{(i)} = MV_{\alpha}(\eta_{\alpha,k}^{(i)}) \\ 0 & \text{otherwise} \end{cases} \quad (0.3.10)$$

Weight Measurement Furthermore, we define the annotators' weights $\omega_{\alpha,k}$ for each class k as the mean of their respective consistency scores $c_{\alpha,k}^{(i)}$ over all instances. The weights are normalized between 0 and 1 as follows:

$$\omega_{\alpha,k} = \frac{\psi_{\alpha,k}}{\sum_{\alpha=1}^M \psi_{\alpha,k}} \quad \text{where} \quad \psi_{\alpha,k} = \frac{1}{N} \sum_{i=1}^N c_{\alpha,k}^{(i)} \quad (0.3.11)$$

LIST OF TABLES—CONTINUED

Aggregated Label Calculation Finally, the aggregated label $v_k^{(i)}$ for each instance i and class k is the weighted average of the predicted labels $\eta_{\alpha,k}^{(i)}$ for each annotator α :

$$v_k^{(i)} = \begin{cases} 1 & \text{if } \left(\sum_{\alpha=1}^M \omega_{\alpha,k} \eta_{\alpha,k}^{(i)} \right) \geq 0.5 \\ 0 & \text{otherwise} \end{cases} \quad \forall i, k \quad (0.3.12)$$

Confidence Score Calculation In previous section we showed how to calculate the aggregated label $v_k^{(i)}$ (shown in Equation (0.3.12)). Define $F_k^{(i)}$ as the confidence score for instance i and class k . In this section, we calculate two confidence scores $F_k^{(i)}$, based on how many different annotators agree on the reported label $v_k^{(i)}$, which will be reported alongside the aggregated label $v_k^{(i)}$. The confidence scores show the level of confidence we should place on the aggregated labels.

To calculate this confidence score, we modify the two techniques used by Sheng [Sheng et al., 2019] and Tao [Tao et al., 2020] to incorporate our calculated weight $\omega_{\alpha,k}$ shown in Equation (0.3.11) for each worker α .

[1.]**uwMV-Freq:** In this approach, the confidence score $F^{(i)}$ is defined as the weighted sum of labels belonging to annotators whose label is the same as the final aggregated label. It is calculated as

$$F_k^{(i)} = \sum_{\alpha=1}^M \omega_{\alpha,k} \delta \left(\eta_{\alpha,k}^{(i)}, v_k^{(i)} \right) \quad (0.3.13)$$

where δ is the Kronecker delta function. **uwMV-Beta:** In this approach, the CDF of the beta distribution at the decision threshold of 0.5 is used to calculate a confidence score $F^{(i)}$. To calculate the two shape parameters of the beta distributions $\alpha^{(i)}$ and $\beta^{(i)}$, we use a weighted sum of all correct and incorrect aggregated labels, respectively:

$$\begin{aligned} l_k^{(i)} &= 1 + \sum_{\alpha=1}^M \omega_{\alpha,k} \delta \left(\eta_{\alpha,k}^{(i)}, v_k^{(i)} \right) \\ u_k^{(i)} &= 1 + \sum_{\alpha=1}^M \omega_{\alpha,k} \delta \left(\eta_{\alpha,k}^{(i)}, 1 - v_k^{(i)} \right) \end{aligned} \quad (0.3.14)$$

$$F_k^{(i)} = I_{0.5} \left(l_k^{(i)}, u_k^{(i)} \right) = \sum_{t=\lfloor l_k^{(i)} \rfloor}^{T-1} \frac{(T-1)!}{t!(T-1-t)!} 0.5^{T-1} \quad (0.3.15)$$

where $T = \lfloor l_k^{(i)} + u_k^{(i)} \rfloor$ and $\lfloor \cdot \rfloor$ is the floor function.

LIST OF TABLES—*CONTINUED***0.4 Results**

In this section, we assess the efficacy of our proposed strategy. To evaluate our proposed technique, we conducted a series of experiments comparing the proposed technique with existing state-of-the-art techniques such as MV, Tao [Tao et al., 2020], and Sheng [Sheng et al., 2019], as well as with other crowdsourcing methodologies reported in the crowd-kit package [?] including Gold Majority Voting, MMSR [Ma and Olshevsky, 2020], Wawa, Zero-Based Skill, GLAD [Whitehill et al., 2009], and Dawid Skene [Dawid and Skene, 1979].

0.4.1 Datasets:

We report the performance of our proposed techniques on various datasets. These datasets cover a wide range of domains and have varying characteristics in terms of the number of features, samples, and class distributions. Table 1 provides an overview of the datasets used. All datasets are obtained from the University of California, Irvine (UCI) repository [Duan and Graff, 2017].

TABLE 1. Descriptions of the datasets used.

Dataset	#Features	#Samples	#Positives	#Negatives
kr-vs-kp	36	3196	1669	1527
mushroom	22	8124	4208	3916
iris	4	100	50	50
spambase	58	4601	1813	2788
tic-tac-toe	10	958	332	626
sick	30	3772	231	3541
waveform	41	5000	1692	3308
car	6	1728	518	1210
vote	16	435	267	168
ionosphere	34	351	126	225

- The **kr-vs-kp** dataset represents the King Rook-King Pawn on a7 in chess. The positive class indicates a victory for white (1,669 instances, or 52%), while the negative class indicates a defeat for white (1,527 instances, 48%).
- The **mushroom** dataset is based on the Audubon Society Field Guide for North American Mushrooms (1981) and includes 21 attributes related to mushroom characteristics such as cap shape, surface, odor, and ring type.

LIST OF TABLES—*CONTINUED*

- The **Iris** Plants Dataset comprises three classes, each with 50 instances, representing different iris plant species. The dataset contains four numerical attributes in centimeters: sepal length, sepal width, petal length, and petal width.
- The **Spambase** dataset consists of 57 attributes, each representing the frequency of a term appearing in an email, such as the “address”.
- The **tic-tac-toe** endgame dataset encodes all possible board configurations for the game, with “x” playing first. It contains nine attributes corresponding to the tic-tac-toe squares: x, o, and b (blank).
- The **Sick** dataset includes thyroid disease records from the Garvan Institute and J. Ross Quinlan of the New South Wales Institute in Sydney, Australia. 3,772 instances with 30 attributes (seven continuous and 23 discrete) and 5.4% missing data. Age, pregnancy, TSH, T3, TT4, etc.
- The **waveform** dataset generator comprises 41 attributes and three wave types, with each class consisting of two “base” waves.
- The **Car** Evaluation Dataset rates cars on price, buying, maintenance, comfort, doors, capacity, luggage, boot size, and safety using a simple hierarchical decision model. The dataset consists of 1,728 instances categorized as unacceptable, acceptable, good, and very good.
- The 1984 US Congressional **Voting** Records Dataset shows how members voted on 16 CQA-identified critical votes. Votes are divided into nine categories, simplified to yea, nay, or unknown disposition. The dataset has two classes: Democrats (267) and Republicans (168).
- The Johns Hopkins **Ionosphere** dataset contains data collected near Goose Bay, Labrador, using a phased array of 16 high-frequency antennas. “Good” radar returns show ionosphere structure, while “bad” returns are ionosphere-free. The dataset includes 351 instances with 34 attributes categorized as good or bad.

All datasets were transformed into a two-class binary problem for comparison with existing benchmarks. For instance, only the first and second classes were used in the “waveform” dataset, and the first two classes were utilized in the “Iris” dataset. In this study, we generated multiple fictitious label sets for each dataset to simulate the crowdsourcing concept of collecting several crowd labels for each instance. This was achieved by selecting random samples in the datasets using a uniform distribution and altering their corresponding true labels to incorrect ones, while maintaining the

LIST OF TABLES—*CONTINUED*

original distribution of the ground-truth labels. The probability of each instance containing the correct true label was determined using a uniform distribution, allowing us to create synthetic label sets for each annotator that preserved the underlying structure and difficulty of the original classification problem. By creating datasets with varying levels of accuracy, we aim to evaluate the performance of our proposed method under different conditions, such as varying annotator expertise and reliability. This process allowed us to assess the ability of our method to handle diverse real-world crowdsourcing scenarios and gain insight into its general applicability and effectiveness in improving overall classification accuracy.

0.4.2 Benchmarks:

Tao [Tao et al., 2020] and Sheng [Sheng et al., 2019] techniques were implemented in Python to evaluate their performance. Furthermore, the crowd-kit package (A General-Purpose Crowdsourcing Computational Quality Control Toolkit for Python) [?] was used to implement the remaining benchmark techniques, including Gold Majority Voting, MMSR [Ma and Olshevsky, 2020], Wawa, Zero-Based Skill, GLAD [Whitehill et al., 2009], and Dawid Skene [Dawid and Skene, 1979].

- **Golden majority voting** estimates the probability that each annotator possesses the correct label and then calculates the probability of each label per occurrence based on the weight assigned to each label. Assume that 10,000 jobs are performed by 3,000 annotators as well as 100 instances of ground truth. First, the percentage of correct labels for each annotator is calculated. The remaining labels were then estimated based on the weights.
- **Wawa** (Annotator Agreement with Aggregate), also referred to as “inter-rater agreement”, is a commonly used statistic for non-testing problems. This indicates the average frequency with which each annotator’s response matches the aggregate response for each instance.
- **Zero-Based-Skill** employs a weighted majority vote (WMV). After processing a collection of instances, it re-evaluated the abilities of the annotators based on the accuracy of their responses. This process is repeated until the labels no longer change or the maximum number of iterations is reached.
- Descriptions of the other techniques can be found in their respective references.

0.4.3 Weight Measurement:

After generating the multi-label sets, we employed both the proposed and state-of-the-art approaches to obtain the aggregated labels. We experimented with two approaches for classifier selection, as explained in Section 3.4.1. We found no significant

LIST OF TABLES—*CONTINUED*

differences in the overall outcomes and thus chose the second approach, which utilized the Random Forest classification technique, to save processing time and reduce the number of required Python package dependencies. Ten Random Forests, each with four trees and a maximum depth of four, were trained in different random states for each annotator α , as detailed in Section 3.

Annotators’ reliability vs estimated weight $\omega_{\alpha,k}$

Figure 0.4.3 depicts the relationship between the randomly assigned annotators’ reliability value ($\pi_{\alpha,k}$) and their corresponding estimated weights, $\omega_{\alpha,k}$. In the case of Tao’s method, the figure displays the average weights across all instances. As seen, when the reliability of an annotator surpasses a specific threshold, the weight measured by Tao’s technique plateaus, whereas the proposed method exhibits a considerably stronger correlation. Individual data points represent the actual measured weights, and the curve represents the regression line.

0.4.4 Confidence-score

The results present a box plot of the average accuracy for different numbers of annotators, ranging from three to ten. Figure 0.4.4 illustrates the average accuracy of the crowd-certain technique with penalization for both the “freq” and “Beta” confidence measurement approaches. A noticeable difference in the accuracy was observed. However, statistical analysis did not reveal a significant difference between these approaches.

Figure 0.4.4 displays the average accuracy using the “freq” confidence measurement strategy for the proposed crowd-certain technique with and without penalization. The penalization method occurs by penalizing annotators for inaccurate labeling before measuring their weights, as demonstrated in Equation (0.3.10). The penalized version of the proposed technique shows an improvement in average accuracy and a reduction in variance.

Figure 0.4.4 shows the average accuracy distribution (“freq” strategy) of the proposed penalized versus Tao and Sheng for a different number of annotators using the kernel density estimation technique. This demonstrates that the proposed technique outperforms both Tao and Sheng on nine of the ten datasets, with higher average accuracy and less fluctuation over different annotator counts. Table 2 shows the statistical data measured between the proposed penalized technique and Tao’s method. As can be seen from these results, the proposed technique has a significant improvement over the seven datasets, while delivering similar results for the other three datasets (p-value < 0.05).

Figure 0.4.4 shows the average accuracy distribution (“Beta” strategy) of the proposed penalized versus Tao and Sheng strategies for different numbers of annotators using kernel density estimation. This demonstrates that the proposed technique out-

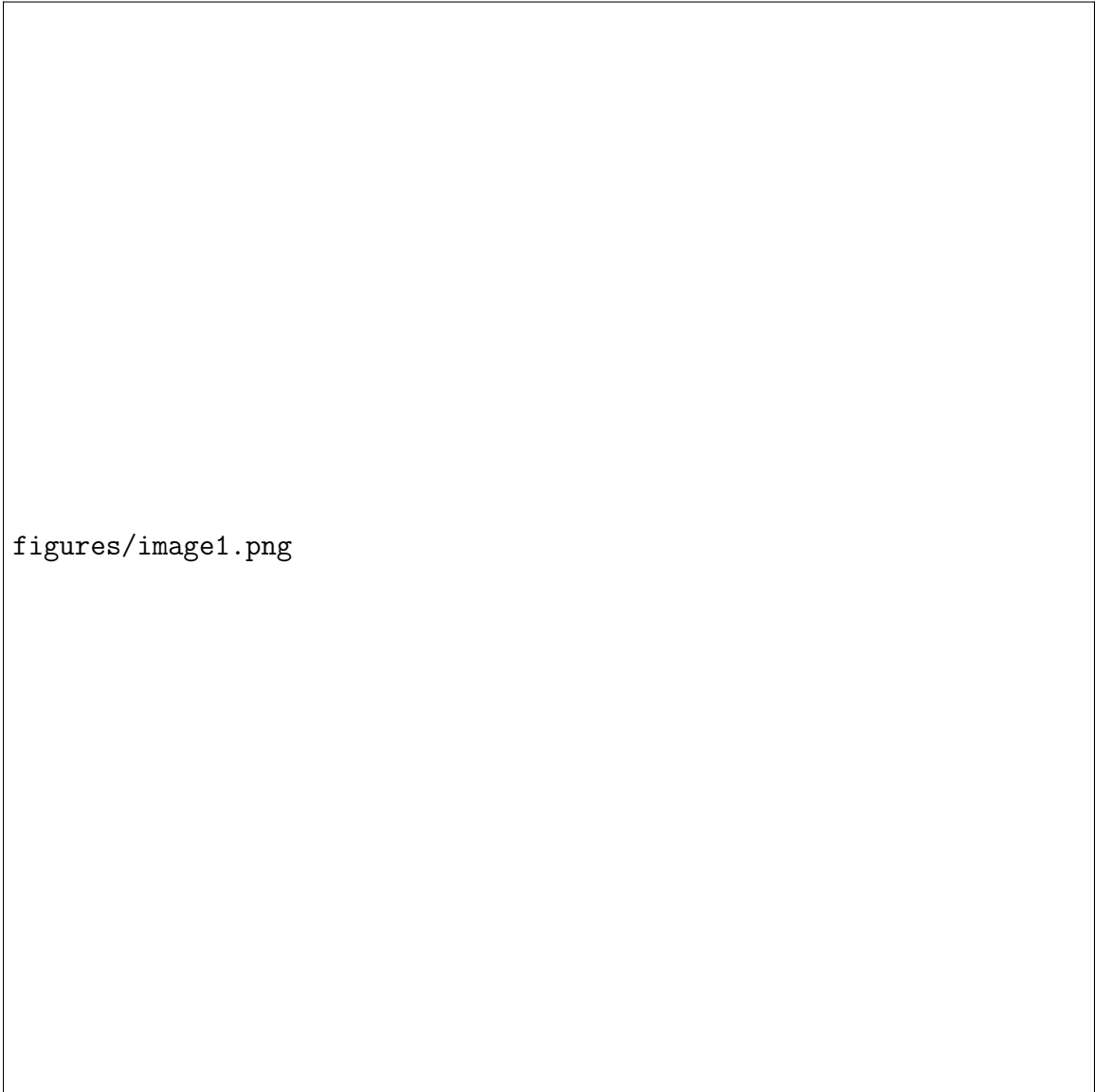
LIST OF TABLES—*CONTINUED*

FIGURE 1. Comparison of estimated weight with respect to annotators' degree of reliability for the proposed aggregation technique "proposed-penalized" and Tao [Tao et al., 2020] for 10 different datasets.

LIST OF TABLES—*CONTINUED*

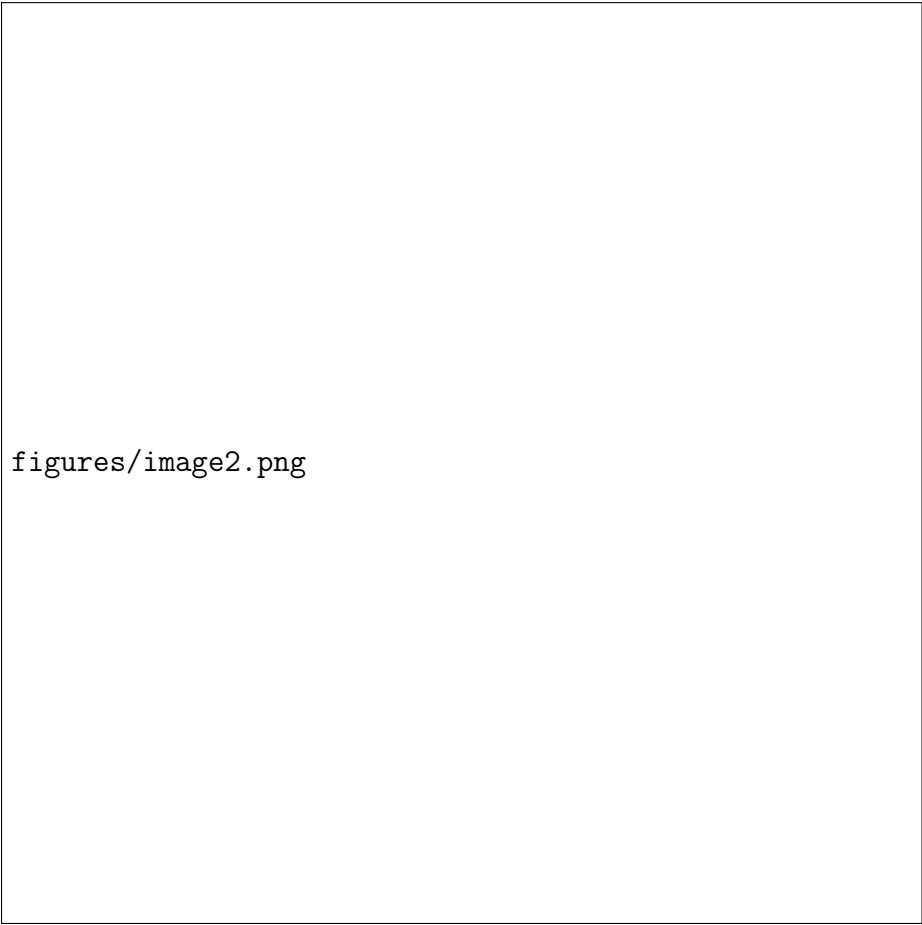


FIGURE 2. Comparison of the measured average accuracy for the two confidence-score measurement techniques in ten different datasets (using the proposed crowd-certain technique with penalization) in different numbers of annotators (from 3 up to 10).

TABLE 2. Statistical tests between the proposed-penalized technique and Tao [Tao et al., 2020] for the ‘freq’ confidence measurement strategy.

Independent t-test	Diff	Degrees of freedom	t	2-sided p-value	Diff<0 p-value	Diff>0 p-value	Cohen d	Hedge’s g	Glass’s delta	Pearson r
Kr-vs-kp	-0.044	12	-6.171	0	0	1	-3.299	-3.088	-2.743	0.872
mushroom	-0.012	12	-2.781	0.017	0.008	0.992	-1.487	-1.392	-1.076	0.626
iris	-0.012	12	-0.506	0.622	0.311	0.689	-0.271	-0.253	-0.226	0.145
spambase	-0.031	12	-3.691	0.003	0.002	0.998	-1.973	-1.847	-1.458	0.729
tic-tac-toe	-0.036	12	-4.612	0.001	0	1	-2.466	-2.308	-2.156	0.8
sick	0.002	12	0.294	0.774	0.613	0.387	0.157	0.147	0.112	0.085
waveform	-0.025	12	-5.118	0	0	1	-2.736	-2.561	-2.022	0.828
car	-0.008	12	-0.779	0.451	0.226	0.774	-0.416	-0.39	-0.309	0.219
vote	-0.033	12	-5.352	0	0	1	-2.861	-2.678	-2.112	0.84
ionosphere	-0.061	12	-6.047	0	0	1	-3.232	-3.026	-2.586	0.868

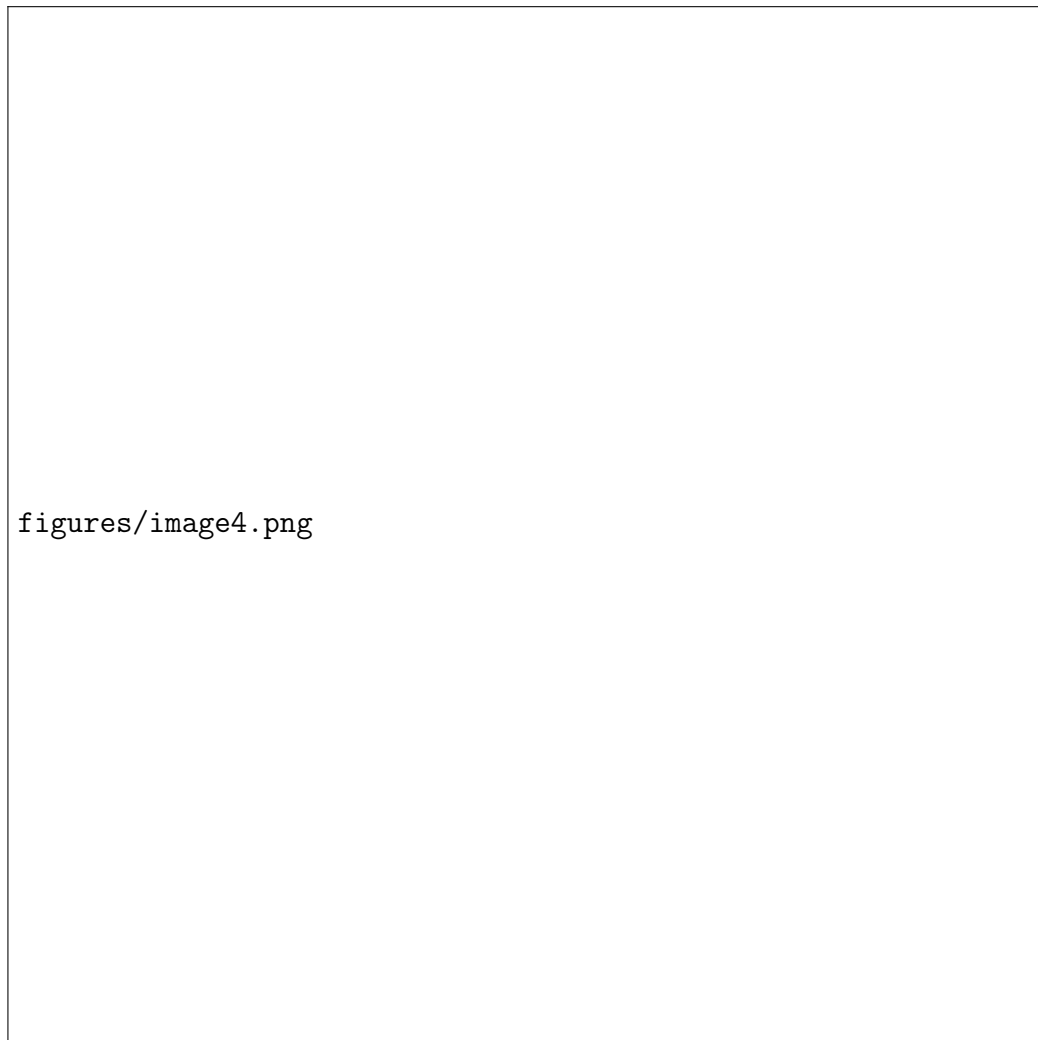
LIST OF TABLES—*CONTINUED*

FIGURE 3. Comparison of the measured average accuracy for the proposed crowd-certain technique with and without penalization and using the ‘freq’ confidence-score strategy on ten different datasets with different numbers of annotators (starting from 3 to 10).

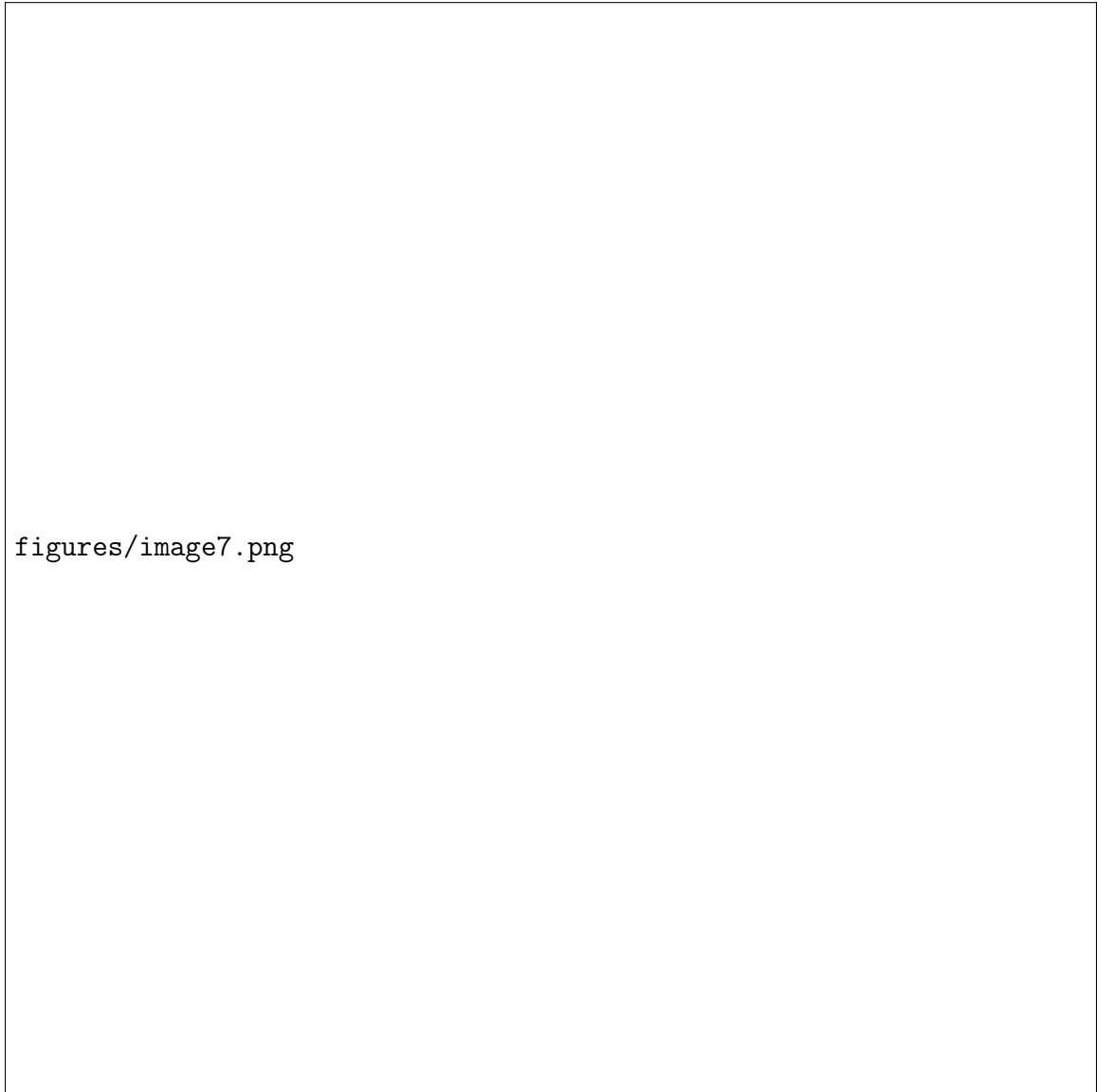
LIST OF TABLES—*CONTINUED*

FIGURE 4. Measured accuracy distribution of the proposed-penalized aggregation technique uwMV-Freq, compared to wMV-Freq (Tao [Tao et al., 2020]), and MV-Freq (Sheng [Sheng et al., 2019]) for different numbers of annotators, using the kernel density estimation technique

LIST OF TABLES—*CONTINUED*

TABLE 3. Statistical tests between the proposed-penalized and Tao [Tao et al., 2020] technique for the “Beta” confidence measurement strategy.

Independent t-test	Diff	Degrees of freedom	t	2-sided p-value	Diff < 0 p-value	Diff > 0 p-value	Cohen d	Hedge’s g	Glass’s delta	Pearson r
kr-vs-kp	-0.04	12	-5.702	0	0	1	-3.048	-2.854	-2.921	0.855
mushroom	-0.009	12	-0.793	0.443	0.222	0.778	-0.424	-0.397	-0.477	0.223
iris	-0.002	12	-0.091	0.929	0.465	0.535	-0.048	-0.045	-0.048	0.026
spambase	-0.03	12	-3.547	0.004	0.002	0.998	-1.896	-1.775	-1.421	0.715
tic-tac-toe	-0.033	12	-4.326	0.001	0	1	-2.312	-2.165	-1.781	0.781
sick	0.001	12	0.14	0.891	0.554	0.446	0.074	0.07	0.053	0.04
waveform	-0.023	12	-2.672	0.02	0.01	0.99	-1.428	-1.337	-1.442	0.611
car	-0.008	12	-0.871	0.401	0.2	0.8	-0.465	-0.436	-0.332	0.244
vote	-0.034	12	-5.198	0	0	1	-2.779	-2.601	-2.081	0.832
ionosphere	-0.052	12	-3.875	0.002	0.001	0.999	-2.071	-1.939	-1.742	0.746

performs both Tao and Sheng on seven out of ten datasets, with higher average accuracy and less fluctuation over different annotator counts. Furthermore, Table 3 shows the statistical data measured between the proposed penalized technique and Tao, showing a significant improvement in six datasets, while performing similarly in the remaining datasets ($p\text{-value} < 0.05$).

Figure 0.4.4 shows the average accuracy for the “ionosphere” dataset for various annotator counts (horizontal axis). As can be seen, the proposed strategies considerably improve accuracy while utilizing a small number of annotators. Furthermore, Figure 0.4.4 shows the average accuracy of the three annotators (the smallest number of annotators that could perform consensus voting) on all ten datasets. Similarly, for the ionosphere dataset, we observed a similar trend in achieving higher accuracy on nine of the ten datasets compared to all benchmarks. It is important to note that the “freq” confidence measurement strategy is used to report the proposed techniques, as well as the Tao and Sheng results. Furthermore, the measured p -value calculated for the measured average accuracy (using three annotators) over different datasets showed a significant improvement for the proposed technique with and without penalization over all remaining benchmarks (Gold Majority Vote, MV, MMSR, Wawa, Zero-Based Skill, GLAD, Dawid Skene).

0.5 Discussion

Label aggregation is a critical component of crowdsourcing and ensemble learning strategies. Many generic label aggregation algorithms fall short because they do not account for the varying reliability of the annotators. In response to this, we have developed a novel label aggregation method that measures annotator reliability based on their consistency and accuracy, in relation to other annotators. We utilized uncertainty estimates to assign each annotator a more accurate weight, which correlates with their agreement with others and their consistency during labeling. In the sec-

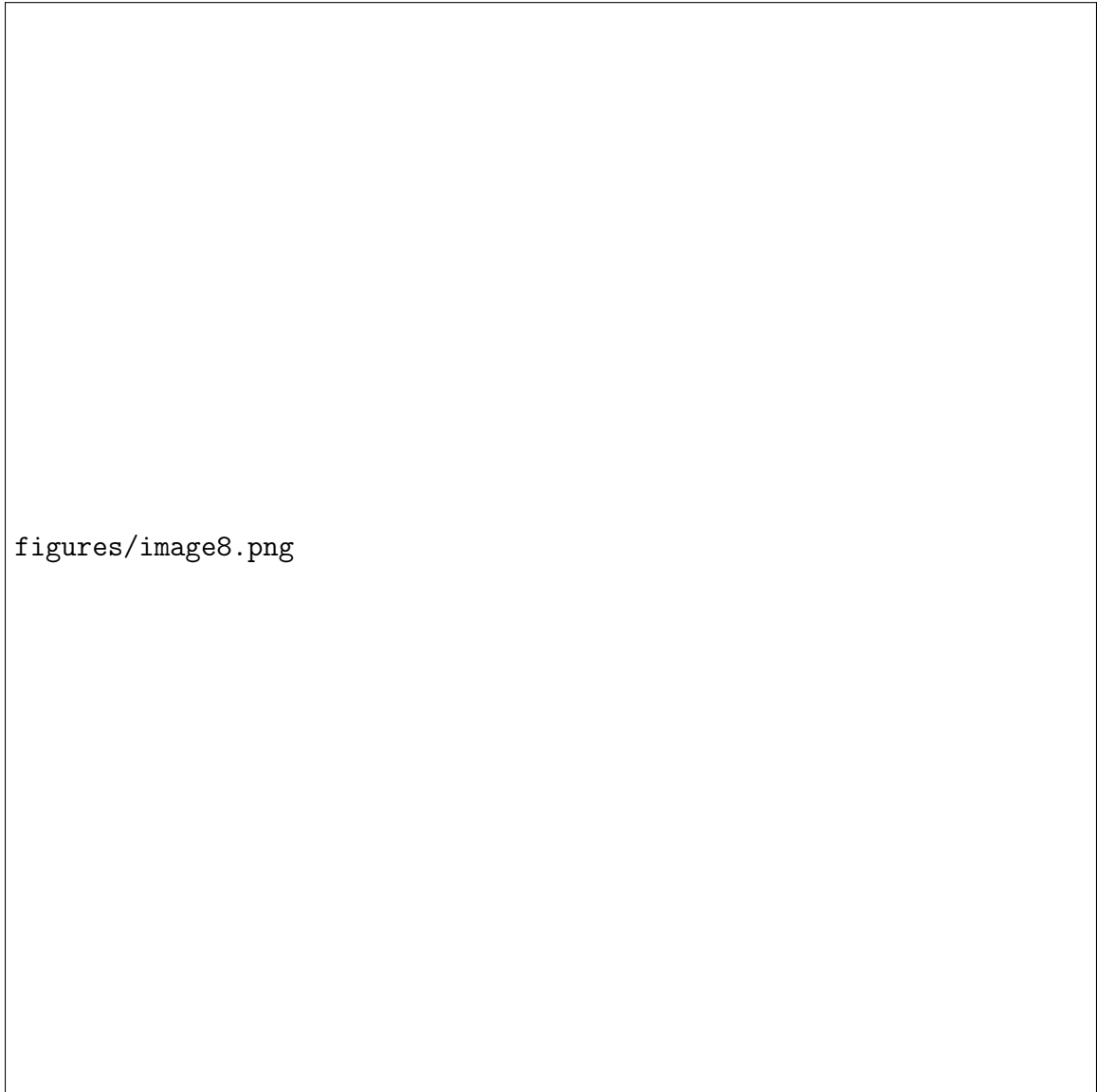
LIST OF TABLES—*CONTINUED*

FIGURE 5. Measured accuracy distribution of the proposed-penalized aggregation technique uwMV-Beta, compared to wMV-Beta (Tao [Tao et al., 2020]), and MV-Beta (Sheng [Sheng et al., 2019]) for different numbers of annotators, using the kernel density estimation technique.

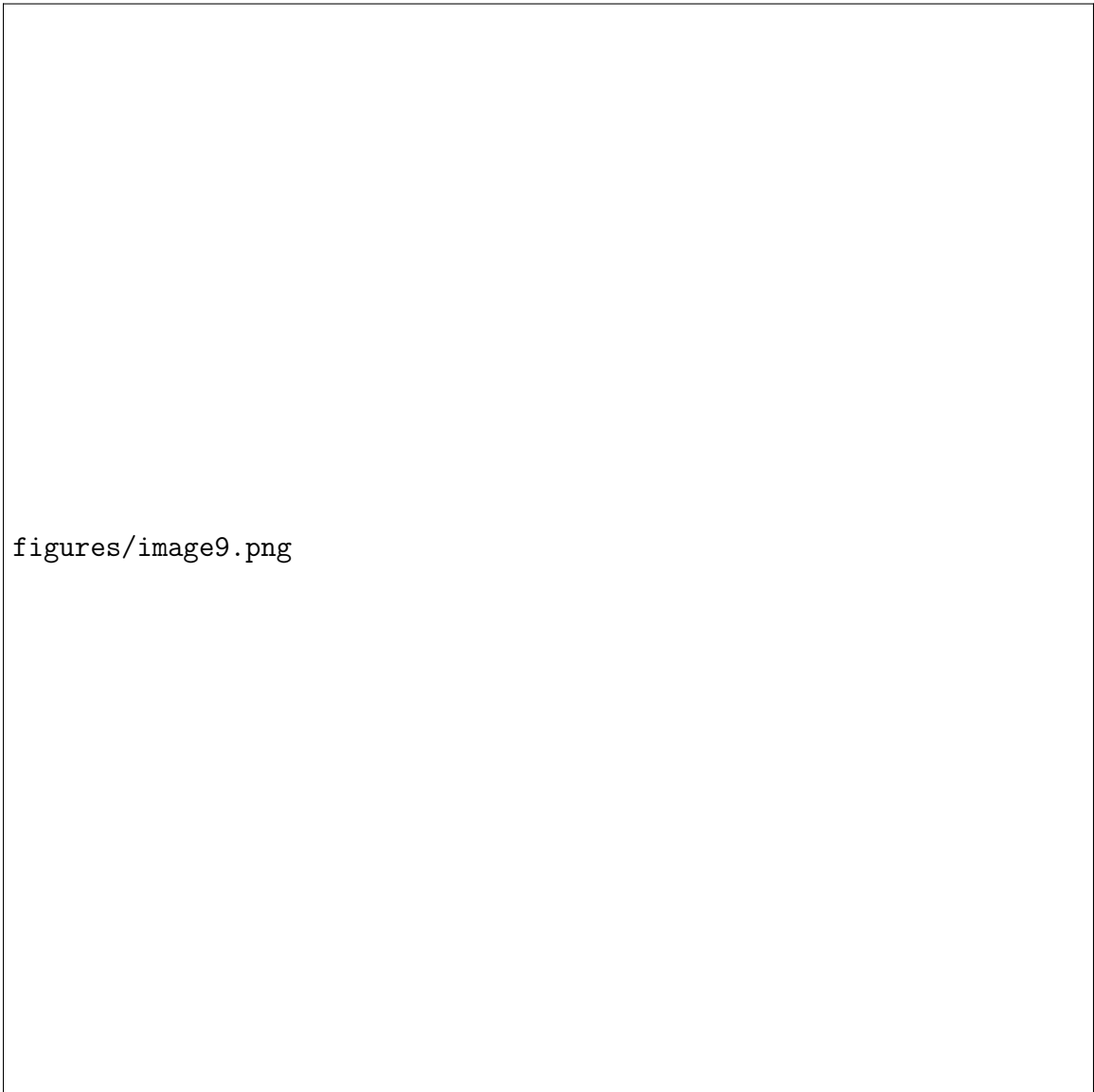
LIST OF TABLES—*CONTINUED*

FIGURE 6. Average accuracy for the proposed aggregation techniques compared to the benchmarks for different numbers of annotators (horizontal axis) in the ionosphere dataset.

LIST OF TABLES—*CONTINUED*

FIGURE 7. Average accuracy of the proposed aggregation techniques compared to the benchmarks for different datasets using three annotators.

LIST OF TABLES—*CONTINUED*

ond approach, we improved our initial strategy by penalizing annotator reliability estimates based on their inconsistencies in labeling. The first part of the proposed algorithm (calculating weights based on consistency) is essential because non-expert annotators often exhibit more irregular consistency during labeling than experts, as they are not trained to identify specific features. This measure helps to differentiate skilled and unskilled annotators. The goal of the second part of the algorithm (penalty for voting against the majority) is to prevent the algorithm from assigning disproportionately high weights to annotators who are consistently incorrect. For example, if annotators consistently mislabel a specific bird species, the second condition penalizes them for their error, despite their consistency. Furthermore, our method reports a single weight for the entire dataset instead of individual weights for each instance. This enables the reuse of calculated weights for future unlabeled test samples without needing to re-acquire labels or retrain classifiers each time new data need labeling. While we have not assessed our method in multi-label scenarios, the proposed techniques are anticipated to perform comparably on multi-label datasets, considering that all steps of the proposed approach involve per-class calculations. Experiments conducted on various crowdsourcing datasets demonstrate that our proposed methods outperform existing techniques in terms of accuracy and variance, especially when there are few annotators available.

0.6 Availability of data and materials

The code can be found in crowd-certain

0.7 Appendices

List of abbreviations

Competing interests

Acknowledgements

REFERENCES

- [Akhondi-Asl et al., 2014] Akhondi-Asl, A., Hoyte, L., Lockhart, M. E., and Warfield, S. K. (2014). A Logarithmic Opinion Pool Based Staple Algorithm for the Fusion of Segmentations With Associated Reliability Weights. *IEEE Trans. Med. Imaging*, 33(10):1997–2009.
- [Angelopoulos and Bates, 2021] Angelopoulos, A. N. and Bates, S. (2021). A Gentle Introduction to Conformal Prediction and Distribution-Free Uncertainty Quantification.
- [Artstein, 2017] Artstein, R. (2017). Inter-Annotator Agreement. In Ide, N. and Pustejovsky, J., editors, *Handbook of Linguistic Annotation*, pages 297–313. Springer Netherlands, Dordrecht.
- [Asman and Landman, 2011] Asman, A. J. and Landman, B. A. (2011). Robust Statistical Label Fusion Through Consensus Level, Labeler Accuracy, and Truth Estimation (COLLATE). *IEEE Trans. Med. Imaging*, 30(10):1779–1794.
- [Asman and Landman, 2012] Asman, A. J. and Landman, B. A. (2012). Formulating Spatially Varying Performance in the Statistical Fusion Framework. *IEEE Trans. Med. Imaging*, 31(6):1326–1336.
- [Asman and Landman, 2013] Asman, A. J. and Landman, B. A. (2013). Non-Local Statistical Label Fusion for Multi-Atlas Segmentation. *Benchmarking Ischemic Stroke Lesion*, 17(2):194–208.
- [Ayhan and Berens, 2018] Ayhan, M. and Berens, P. (2018). Test-Time Data Augmentation for Estimation of Heteroscedastic Aleatoric Uncertainty in Deep Neural Networks. In *1st Conference on Medical Imaging with Deep Learning*.
- [Bi et al., 2014] Bi, W., Wang, L., Kwok, J. T., and Tu, Z. (2014). Learning to Predict From Crowdsourced Data. In *Proc. 13th Conf. Uncertain. Artif. Intell.*, UAI’14, pages 82–91, Arlington, Virginia, USA. AUAI Press.
- [Carletta, 1996] Carletta, J. (1996). Assessing Agreement on Classification Tasks: The Kappa Statistic. *Comput. Linguist.*, 22(2):249–254.
- [Commowick et al., 2018] Commowick, O., Istace, A., Kain, M., Laurent, B., Leray, F., Simon, M., Pop, S. C., Girard, P., Améli, R., Ferré, J.-C., Kerbrat, A., Tourdias, T., Cervenansky, F., Glatard, T., Beaumont, J., Doyle, S., Forbes, F., Knight, J., Khademi, A., Mahbod, A., Wang, C., McKinley, R., Wagner, F., Muschelli, J., Sweeney, E., Roura, E., Lladó, X., Santos, M. M., Santos, W. P., Silva-Filho,

- A. G., Tomas-Fernandez, X., Urien, H., Bloch, I., Valverde, S., Cabezas, M., Vera-Olmos, F. J., Malpica, N., Guttmann, C., Vukusic, S., Edan, G., Dojat, M., Styner, M., Warfield, S. K., Cotton, F., and Barillot, C. (2018). Objective Evaluation of Multiple Sclerosis Lesion Segmentation Using a Data Management and Processing Infrastructure. *Sci Rep*, 8(1):13650.
- [Dalvi et al., 2013] Dalvi, N., Dasgupta, A., Kumar, R., and Rastogi, V. (2013). Aggregating Crowdsourced Binary Ratings. In *Proc. 22nd Int. Conf. World Wide Web*, WWW '13, pages 285–294, New York, NY, USA. Association for Computing Machinery.
- [Dawid and Skene, 1979] Dawid, A. P. and Skene, A. M. (1979). Maximum Likelihood Estimation of Observer Error-Rates Using the EM Algorithm. *Applied Statistics*, 28(1):20.
- [Demartini et al., 2012] Demartini, G., Difallah, D. E., and Cudré-Mauroux, P. (2012). Zencrowd: Leveraging Probabilistic Reasoning and Crowdsourcing Techniques for Large-Scale Entity Linking. In *Proc. 21st Int. Conf. World Wide Web*, pages 469–478, Lyon France. ACM.
- [Deng et al., 2009] Deng, J., Dong, W., Socher, R., Li, L.-J., Kai Li, and Li Fei-Fei (2009). ImageNet: A Large-Scale Hierarchical Image Database. In *Conf. Comput. Vis. Pattern Recognit.*, pages 248–255, Miami, FL. IEEE.
- [Duan and Graff, 2017] Duan, D. and Graff, C. (2017). UCI Machine Learning Repository.
- [Eugenio Iglesias et al., 2013] Eugenio Iglesias, J., Rory Sabuncu, M., and Van Leemput, K. (2013). A Unified Framework for Cross-Modality Multi-Atlas Segmentation of Brain Mri. *Medical Image Analysis*, 17(8):1181–1191.
- [Gal and Ghahramani, 2016] Gal, Y. and Ghahramani, Z. (2016). Dropout as a Bayesian Approximation: Representing Model Uncertainty in Deep Learning. In *Proc. 33rd Int. Conf. Mach. Learn.*, pages 1050–1059. PMLR.
- [Ghosh et al., 2011] Ghosh, A., Kale, S., and McAfee, P. (2011). Who Moderates the Moderators?: Crowdsourcing Abuse Detection in User-Generated Content. In *Proc. 12th ACM Conf. Electron. Commer.*, page 167, San Jose, California, USA. ACM Press.
- [Hernandez-Gonzalez et al., 2019] Hernandez-Gonzalez, J., Inza, I., and Lozano, J. A. (2019). A Note on the Behavior of Majority Voting in Multi-Class Domains With Biased Annotators. *IEEE Trans. Knowl. Data Eng.*, 31(1):195–200.

- [Hoeting et al., 1999] Hoeting, J. A., Madigan, D., Raftery, A. E., and Volinsky, C. T. (1999). Bayesian Model Averaging: A Tutorial (With Comments by M. Clyde, David Draper and E. I. George, and a Rejoinder by the Authors. *Statist. Sci.*, 14(4).
- [Jiang et al., 2019a] Jiang, L., Kong, G., and Li, C. (2019a). Wrapper Framework for Test-Cost-Sensitive Feature Selection. *IEEE Trans. Syst. Man Cybern, Syst.*, pages 1–10.
- [Jiang et al., 2019b] Jiang, L., Zhang, L., Yu, L., and Wang, D. (2019b). Class Specific Attribute Weighted Naive Bayes. *Pattern Recognition*, 88:321–330.
- [Jorge Cardoso et al., 2013] Jorge Cardoso, M., Leung, K., Modat, M., Keihaninejad, S., Cash, D., Barnes, J., Fox, N. C., and Ourselin, S. (2013). STEPS: Similarity and Truth Estimation for Propagated Segmentations and Its Application to Hippocampal Segmentation and Brain Parcelation. *Medical Image Analysis*, 17(6):671–684.
- [Karger et al., 2014] Karger, D. R., Oh, S., and Shah, D. (2014). Budget Optimal Task Allocation for Reliable Crowdsourcing Systems. *Operations Research*, 62(1):1–24.
- [Krippendorff, 2018] Krippendorff, K. (2018). *Content Analysis: An Introduction to Its Methodology*. SAGE, Los Angeles, fourth edition edition.
- [Kurve et al., 2015] Kurve, A., Miller, D. J., and Kesidis, G. (2015). Multi-Category Crowdsourcing Accounting for Variable Task Difficulty, Worker Skill, and Worker Intention. *IEEE Trans. Knowl. Data Eng.*, 27(3):794–809.
- [Li et al., 2019] Li, C., Jiang, L., and Xu, W. (2019). Noise Correction to Improve Data and Model Quality for Crowdsourcing. *Engineering Applications of Artificial Intelligence*, 82:184–191.
- [Li et al., 2016] Li, C., Sheng, V. S., Jiang, L., and Li, H. (2016). Noise Filtering to Improve Data and Model Quality for Crowdsourcing. *Knowledge-Based Systems*, 107:96–103.
- [Li et al., 2017] Li, G., Zheng, Y., Fan, J., Wang, J., and Cheng, R. (2017). Crowdsourced Data Management: Overview and Challenges. In *Proc. 2017 ACM Int. Conf. Manag. Data*, pages 1711–1716, Chicago Illinois USA. ACM.
- [Li et al., 2018] Li, J., Baba, Y., and Kashima, H. (2018). Incorporating Worker Similarity for Label Aggregation in Crowdsourcing. In *Artificial Neural Networks and Machine Learning (ICANN)*, volume 11140 of *Lecture Notes in Computer Science*, pages 596–606, Cham. Springer International Publishing.

- [Liu et al., 2021] Liu, J., Tang, F., Chen, L., and Zhu, Y. (2021). Exploiting Predicted Answer in Label Aggregation to Make Better Use of the Crowd Wisdom. *Information Sciences*, 574:66–83.
- [Liu et al., 2017] Liu, M., Jiang, L., Liu, J., Wang, X., Zhu, J., and Liu, S. (2017). Improving Learning-From-Crowds Through Expert Validation. In *Proc. 26th Int. Jt. Conf. Artif. Intell.*, pages 2329–2336, Melbourne, Australia.
- [Liu et al., 2012] Liu, Q., Peng, J., and Ihler, A. T. (2012). Variational Inference for Crowdsourcing. In *Adv. Neural Inf. Process. Syst.*, volume 25. Curran Associates, Inc.
- [Ma and Olshevsky, 2020] Ma, Q. and Olshevsky, A. (2020). Adversarial Crowdsourcing Through Robust Rank-One Matrix Completion. In *Adv. Neural Inf. Process. Syst.*, volume 33, pages 21841–21852. Curran Associates, Inc.
- [Ma et al., 2020] Ma, Y., Olshevsky, A., Saligrama, V., and Szepesvari, C. (2020). Gradient Descent for Sparse Rank-One Matrix Completion for Crowd-Sourced Aggregation of Sparsely Interacting Workers. *J. Mach. Learn. Res.*, 21(1):5245–5280.
- [Mullachery et al., 2018] Mullachery, V., Khera, A., and Husain, A. (2018). Bayesian Neural Networks.
- [Raykar et al., 2010] Raykar, V. C., Yu, S., Zhao, L. H., Valadez, G. H., Florin, C., Bogoni, L., Moy, L., Raykar, C., Valadez, G. H., Florin, C., Bogoni, L., and Moy, L. (2010). Learning From Crowds. *JMLR*, 11(43):1297–1322.
- [Sheng et al., 2019] Sheng, V. S., Zhang, J., Gu, B., and Wu, X. (2019). Majority Voting and Pairing With Multiple Noisy Labeling. *IEEE Trans. Knowl. Data Eng.*, 31(7):1355–1368.
- [Sheshadri and Lease, 2013] Sheshadri, A. and Lease, M. (2013). SQUARE: A Benchmark for Research on Computing Crowd Consensus. *HCOMP*, 1:156–164.
- [Tao et al., 2020] Tao, F., Jiang, L., and Li, C. (2020). Label Similarity-Based Weighted Soft Majority Voting and Pairing for Crowdsourcing. *Knowl Inf Syst*, 62(7):2521–2538.
- [Tian et al., 2019] Tian, T., Zhu, J., and Qiaoben, Y. (2019). Max-Margin Majority Voting for Learning From Crowds. *IEEE Trans. Pattern Anal. Mach. Intell.*, 41(10):2480–2494.
- [Tu et al., 2018] Tu, J., Yu, G., Domeniconi, C., Wang, J., Xiao, G., and Guo, M. (2018). Multi-Label Answer Aggregation Based on Joint Matrix Factorization. In *2018 IEEE Int. Conf. Data Min. ICDM*, pages 517–526, Singapore. IEEE.

- [Vapnik, 1991] Vapnik, V. (1991). Principles of Risk Minimization for Learning Theory. In *Adv. Neural Inf. Process. Syst.*, volume 4. Morgan-Kaufmann.
- [Wang et al., 2020] Wang, X., Kondratyuk, D., Christiansen, E., Kitani, K. M., Alon, Y., and Eban, E. (2020). Wisdom of Committees: An Overlooked Approach to Faster and More Accurate Models.
- [Warfield et al., 2004] Warfield, S., Zou, K., and Wells, W. (2004). Simultaneous Truth and Performance Level Estimation (STAPLE): An Algorithm for the Validation of Image Segmentation. *IEEE Trans. Med. Imaging*, 23(7):903–921.
- [Welinder et al., 2010] Welinder, P., Branson, S., Perona, P., and Belongie, S. (2010). The Multidimensional Wisdom of Crowds. In *Adv. Neural Inf. Process. Syst.*, volume 23. Curran Associates, Inc.
- [Whitehill et al., 2009] Whitehill, J., Wu, T.-f., Bergsma, J., Movellan, J., and Ruvolo, P. (2009). Whose Vote Should Count More: Optimal Integration of Labels From Labelers of Unknown Expertise. In *Adv. Neural Inf. Process. Syst.*, volume 22. Curran Associates, Inc.
- [Winzeck et al., 2018] Winzeck, S., Hakim, A., McKinley, R., Pinto, J. A. A. D. S. R., Alves, V., Silva, C., Pisov, M., Krivov, E., Belyaev, M., Monteiro, M., Oliveira, A., Choi, Y., Paik, M. C., Kwon, Y., Lee, H., Kim, B. J., Won, J.-H., Islam, M., Ren, H., Robben, D., Suetens, P., Gong, E., Niu, Y., Xu, J., Pauly, J. M., Lucas, C., Heinrich, M. P., Rivera, L. C., Castillo, L. S., Daza, L. A., Beers, A. L., Arbelaez, P., Maier, O., Chang, K., Brown, J. M., Kalpathy-Cramer, J., Zaharchuk, G., Wiest, R., and Reyes, M. (2018). ISLES 2016 and 2017-Benchmarking Ischemic Stroke Lesion Outcome Prediction Based on Multispectral MRI. *Front. Neurol.*, 9:679.
- [Zhang et al., 2019] Zhang, J., Sheng, V. S., and Wu, J. (2019). Crowdsourced Label Aggregation Using Bilayer Collaborative Clustering. *IEEE Trans. Neural Netw. Learning Syst.*, 30(10):3172–3185.
- [Zhang and Wu, 2018] Zhang, J. and Wu, X. (2018). Multi-Label Inference for Crowdsourcing. In *Proc. 24th ACM SIGKDD Int. Conf. Knowl. Discov. Data Min.*, pages 2738–2747, London United Kingdom. ACM.
- [Zhang et al., 2013] Zhang, J., Wu, X., and Sheng, V. (2013). Imbalanced Multiple Noisy Labeling for Supervised Learning. In *Proc. AAAI Conf. Artif. Intell.*, volume 27, pages 1651–1652.
- [Zhang et al., 2014] Zhang, Y., Chen, X., Zhou, D., and Jordan, M. I. (2014). Spectral Methods Meet EM: A Provably Optimal Algorithm for Crowdsourcing. In *Adv. Neural Inf. Process. Syst.*, volume 27, pages 1260–1268. Curran Associates, Inc.

~~LIST OF TABLES~~ ~~CONTINUED~~
[Zheng et al., 2017] Zheng, Y., Li, G., Li, Y., Shan, C., and Cheng, R. (2017).
Truth Inference in Crowdsourcing: Is the Problem Solved? *Proc. VLDB Endow.*,
10(5):541–552.